Eur. J. Mech. B - Fluids 19 (2000) 1–22

Resemblance of K- and N-regimes of boundary-layer transition at late stages

Sebastian Bake [a,*], Hans H. Fernholz [a], Yury S. Kachanov [b]

[a] *Hermann-Föttinger-Institut für Strömungsmechanik, Technische Universität Berlin, Straße des 17. Juni 135, 10623 Berlin, Germany*
[b] *Institut for Theoretical and Applied Mechanics, Russian Academy of Science, 630090 Novosibirsk, Russia*

(Received 7 May 1998; revised 15 January 1999; accepted 16 March 1999)

Abstract – This paper is devoted to an experimental study of late nonlinear stages of laminar–turbulent transition in a 2D flow close to the Blasius boundary-layer. The measurements were conducted at controlled disturbance conditions with excitation of a 2D large-amplitude fundamental instability wave with frequency f_1 and/or a pair of low-amplitude oblique subharmonic instability waves with frequency $f_1/2$ and values of the spanwise wavenumber $\pm\beta_{1/2}$. In the case with a phase shift between the fundamental mode and the pair of the subharmonics favourable for the subharmonic resonance the transition process was found to be characterised by a rapid resonance growth of the 3D subharmonic modes. This was followed by a formation of the Λ-structures within each subharmonic period in time, positioned in a staggered order in space that is typical of the N-regime (or the subharmonic regime) of the boundary layer breakdown. However, at late stages of the disturbance development the local behaviour of the perturbations in the vicinity of the Λ-structures turned out to be very similar to that typically observed in the K-regime of breakdown. This could be seen in the formation of an intensive Λ-shaped 3D high-shear layer and the coherent structures associated with spikes in the time-traces of the hot-wire signal. Sets of consecutive spikes were found to be generated in the vicinity of the tip of each Λ-structure. The arrays of spikes had also the staggered order with the streamwise and spanwise spacing characteristic of the subharmonic wave (as in the N-regime) but their local properties were found to be qualitatively the same as those typical for the K-regime. Despite the significantly different nature of the initial stages of these two scenarios of transition, described usually in terms of weakly nonlinear interactions of the instability waves, the late stages of these two types of breakdown (described usually in terms of vortices attributed to the coherent structures) have approximately the same physical nature. © 2000 Éditions scientifiques et médicales Elsevier SAS

K-regime / N-regime / transitional Lambda-structures

1. Introduction

The nonlinear stage of the laminar–turbulent transition in a boundary-layer is the last phase of a sequence of phenomena attributed to the transition process. In contrast to the preceding linear stages, many aspects of the nonlinear stage are still unclear. In a relatively short spatial region where the disturbance amplitudes are of an order of 1% of the free-stream velocity or more, the flow transforms rather rapidly from a deterministic laminar flow into a stochastic turbulent one.

In the case of not very high levels of external perturbations a so-called ‘normal’ class of the transition scenarios is realized (in contrast to another class of scenarios usually called ‘bypass’ transition). In this case two main regimes of the 2D boundary-layer breakdown have been identified and investigated experimentally: first the K-regime (after Klebanoff et al. [1]) and second the N-regime found by Kachanov et al. [2]. Very often the latter is also called the ‘subharmonic regime’ (see e.g. Zelman and Maslennikova [3]) or the ‘H-regime’ (more frequently: the ‘H-mode of secondary instability’ or the ‘H-type of interaction the instability waves’) after Herbert [4] who has developed the Floquet theory for the description of the initial stages of the N-regime of transition. (Note also that there are several other (theoretically) possible scenarios of transition in the Blasius boundary layer which, however, have not yet been studied experimentally although they can exist in nature.) For

* Correspondence and reprints; bake@pi.tu-berlin.de

simplicity of discussion we concentrate here on a case when the primary instability wave entering the nonlinear region is periodic in time; although this restriction is not very significant, as it has been shown in several recent investigations. The K-regime is observed at relatively high levels of the fundamental 2D instability wave and relatively low levels of the low-frequency background fluctuations near the subharmonic frequency, while the N-regime occurs in the opposite situation (Saric et al. [5]). (Note meanwhile, that the K-regime of breakdown represents a rather universal scenario and can be observed in different flows, in particular in some cases of bypass transition when the initial disturbance amplitudes are very high from the very beginning.)

The K-regime has been studied in many experimental investigations (see for instance Hama [6], Klebanoff et al. [1], Kovasznay et al. [7], Hama and Nutant [8], Knapp and Roach [9], Kachanov et al. [10], Saric and Thomas [11], Saric et al. [5], Kachanov [12], Borodulin and Kachanov [13,14], Dryganets et al. [15], Borodulin and Kachanov [16,17]). Some theoretical approaches towards understanding the physical mechanisms of the K-breakdown were discussed for example by Craik [18,19], Nayfeh [20], Herbert [21], Rist [22], Kleiser and Zang [23], Kachanov et al. [24], Kachanov [25], Rist and Fasel [26], Rist and Kachanov [27] and others. The flow in this regime remains deterministic (periodic) until rather a late stage of the transition. The K-regime has the following characteristic features:

(a) growth of the 3D instability modes at the fundamental ($f = f_1$) and zero frequencies (mean flow deformation);
(b) formation of pulsating streamwise vortices and growth of spanwise modulation of the mean velocity and the disturbance amplitudes (and phases) leading to the formation of 'peaks' and 'valleys' in the spanwise distributions, with very high amplitudes of the perturbations in the peak positions;
(c) rapid (but not explosive) growth of the 3D high-frequency spectral modes ($nf_1, \pm m\beta_1$) (where $n, m = 0, 1, 2, 3, \ldots$ and β_1 is the fundamental spanwise wavenumber) and synchronisation of their phases in time and space;
(d) formation of Λ-structures (at each period of the fundamental wave) aligned in rows consisting mainly of a permanently deforming vortex loop (Λ-vortex) and a 3D (also Λ-shaped) high-shear layer;
(e) continuous stretching of the Λ-structures and concentration of the vorticity in the 'legs' of the Λ-vortex;
(f) appearance of very intensive flashes in the streamwise-velocity time traces called 'spikes' which are doubled, tripled, etc. in downstream direction;
(g) multiple reconnection of the Λ-vortex 'legs' near its tip and formation of the ring-like vortices (through an intermediate stage of the Ω-vortices, or the hair-pin vortices) which represent very stable, soliton-like coherent structures (called the *CS*-solitons). They have very conservative (slow dissipation) properties and are closely connected with the spikes;
(h) growth of quasi-random, non-periodic perturbations (first of all around the frequencies $f_{n/2} = nf_1/2$, where $n = 1, 2, 3, \ldots$), phased-locked with the fundamental wave, observed in the near-wall region in a vicinity of the peak position and a complete randomisation of the flow in this local region.

The N-regime of transition has been investigated experimentally in detail, especially its early stages (see for instance Knapp and Roach [9], Kachanov et al. [2], Kachanov and Levchenko [28], Saric and Thomas [11], Saric et al. [5], Corke and Mangano [29], Corke [30], Corke and Gruber [31], Bake et al. [32], and others). Some theoretical aspects of the physical mechanisms of the initial stages of this regime were discussed by Craik [18,19], Nayfeh [20], Smith and Stewart [33], Herbert [21], Fasel [34], Kleiser and Zang [23], Zelman and Maslennikova [3], Goldstein [35], Kachanov [25], for example. Note that first theoretical approaches which where able to explain the N-regime of transition observed in experiments by Kachanov et al. [10] and Kachanov and Levchenko [28] (published as a preprint in 1982) were a weakly-nonlinear theory by Volodin and Zelman [36] and Zelman and Maslennikova [37] (based on ideas of Craik [18] and linear Floquet theory by Herbert [38]. Some misunderstandings between the two approaches have been clarified by Zelman and

Maslennikova [3]. The N-regime of transition can be subdivided into two somewhat different sub-regimes: (i) with random initial quasi-subharmonic perturbations and (ii) with regular (sinusoidal) initial subharmonic perturbations. There is one more case of the N-breakdown with the presence of detuned periodic quasi-subharmonic waves in the initial disturbance spectrum (studied by Kachanov and Levchenko [28], Corke [30, 39]) that represents just an intermediate case simulating a mechanism of amplification of the random quasi-subharmonic modes observed in the sub-regime (i).

In sub-regime (i) the flow in the N-regime of transition is characterised by the following features:

(a) rapid resonant amplification of the 3D instability modes in a wide low-frequency range around the subharmonic frequency $f_{1/2} = f_1/2$, and also around the modes $f_{n/2} = nf_1/2$ ($n = 3, 5, 7, \ldots$), with 'resonant' values of the spanwise wavenumber;
(b) formation of groups of weak ('primary', Hama and Nutant [8]) Λ-structures with their quasi-periodicity in time (inside every group) characteristic of the subharmonic wave and with their staggered-like order in space;
(c) subsequent growth of the quasi-subharmonic, low-frequency perturbations and the disturbances around the frequencies $f_{n/2} = nf_1/2$ ($n = 3, 5, 7, \ldots$), a gradual broadband filling of the disturbance spectrum, and a final randomisation of the flow.

In sub-regime (ii) the flow in the N-regime of transition is characterised by the following features:

(a) rapid resonant amplification of a pair of the 3D instability modes with the subharmonic frequency $f_{1/2} = f_1/2$ and with frequencies $f_{n/2} = nf_1/2$ ($n = 3, 5$ with 'resonant' values of the spanwise wavenumber ($\beta = \pm\beta_{r1/2}$ for the subharmonics);
(b) formation of weak ('primary') Λ-structures positioned in a staggered order with periodicity $1/f_{1/2}$ in time and $2\pi/\beta_{r1/2}$ in space;
(c) saturation of the growth of the subharmonic waves reached at very high amplitudes (much greater than the fundamental one), a gradual broadband filling of the disturbance spectrum and a final breakdown of the flow.

As can be seen from a comparison of the lists of characteristic features of the K- and N-regimes of breakdown, the K-regime has been studied in much more detail as compared to the N-regime. In the latter case the initial stages have been investigated thoroughly but the late stages are relatively unclear. In particular, the mechanisms of the evolution and breakdown of the 'primary' Λ-structures need to be studied. For instance, a high-shear layer represents an inherent property of the developed Λ-structures observed in the K-regime of transition (see e.g. Hama and Nutant [8], Kovasznay et al. [7], Kachanov et al. [10], Borodulin and Kachanov [17] and Rist and Fasel [26]. However, as was mentioned by Corke and Gruber [31] the high-shear layers have never been observed in the subharmonic regime of transition in the Blasius flow; this is generally a characteristic feature of the K-regime. This phenomenon was detected by them (and also by Kloker [40] in the DNS) in the adverse-pressure gradient flow only when a subharmonic-like regime of transition was simulated. Corke and Gruber [31] suggested that the main reason for this is a rapid growth of the fundamental wave and its high initial amplitude. One of the most characteristic features of the K-regime (observed at subsequent stages of development of the Λ-structure) is the appearance of spikes, i.e. of very intensive flashes of the streamwise component of the velocity fluctuations. This phenomenon has also never been observed in the N-regime of transition including its late stages (see for instance Corke and Mangano [29] and Corke [30]). As it was suggested by Corke and Gruber [31], one of possible reason for absence of spikes in the previous experiments devoted to investigations of late stages of the N-regime of breakdown was the rather low initial amplitudes of the fundamental wave. Based on DNS results obtained for the Blasius flow, Laurien and Kleiser [41] also indicated that there is a possibility that the breakdown of Λ-vortices in the N-regime might occur in a similar way as in the K-regime if the initial amplitude of the subharmonic is high enough. This question was also

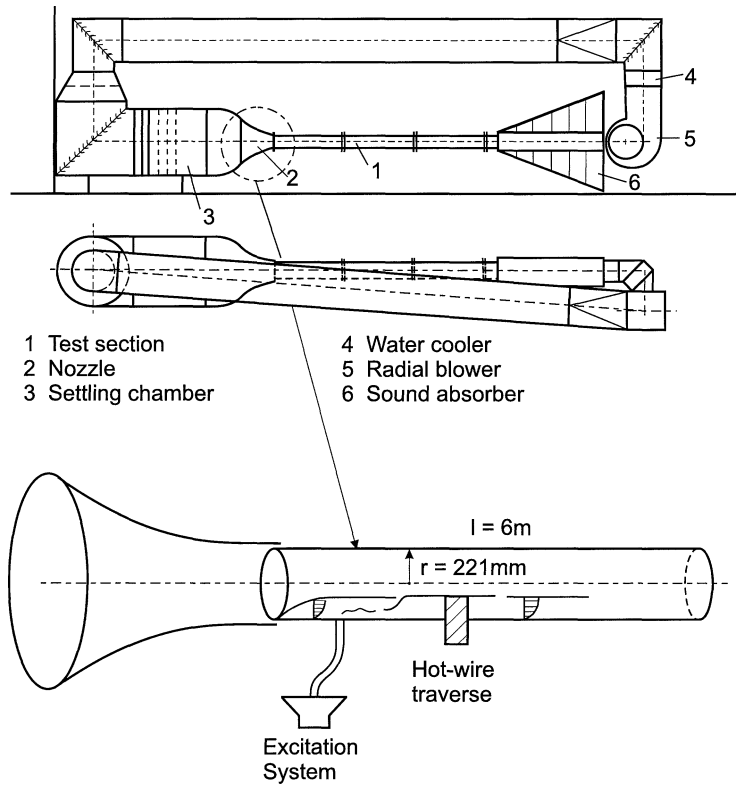

Figure 1. Sketch of the laminar wind tunnel with measurement section at HFI.

discussed by Kachanov [25] together with an analogy between the physical mechanisms of the K-regime of transition and the structure of the developed turbulent boundary layer. It was noted by Kachanov [25] that either there are two different types of the near-wall turbulence (i.e. the K-turbulence and the N-turbulence), which is almost impossible, or "...possibly, a mechanism of spike formation similar to that observed in the K-regime can begin to work at a certain late stage of the N-breakdown...". The main goal of the present study was to investigate this possibility experimentally and to clarify the main physical mechanisms of the late stages of the N-regime of boundary-layer breakdown.

2. Experimental procedure

2.1. The wind tunnel and basic flow

The experiment was conducted in the Laminar Wind Tunnel of the Hermann-Föttinger-Institute of Berlin Technical University. It is a closed-circuit tunnel with an axisymmetric test section made of Plexiglas tubes with an inner diameter of 441 mm and a total length of 6000 mm. This wind-tunnel has a nozzle contraction-ratio 18 : 1 over a length of 2 m and the boundary-layer of the nozzle is blown out. The boundary-layer under investigation starts at the elliptic leading edge of the test section and develops downstream on its inner wall (*figure 1*). Because of the axisymmetric shape of the test section no side-wall effects occur. The wind tunnel has a main radial fan with a 15 kW motor and an additional blower to supply inside the pressure for blowing out the nozzle boundary-layer. The flow temperature can be controlled with a water cooler.

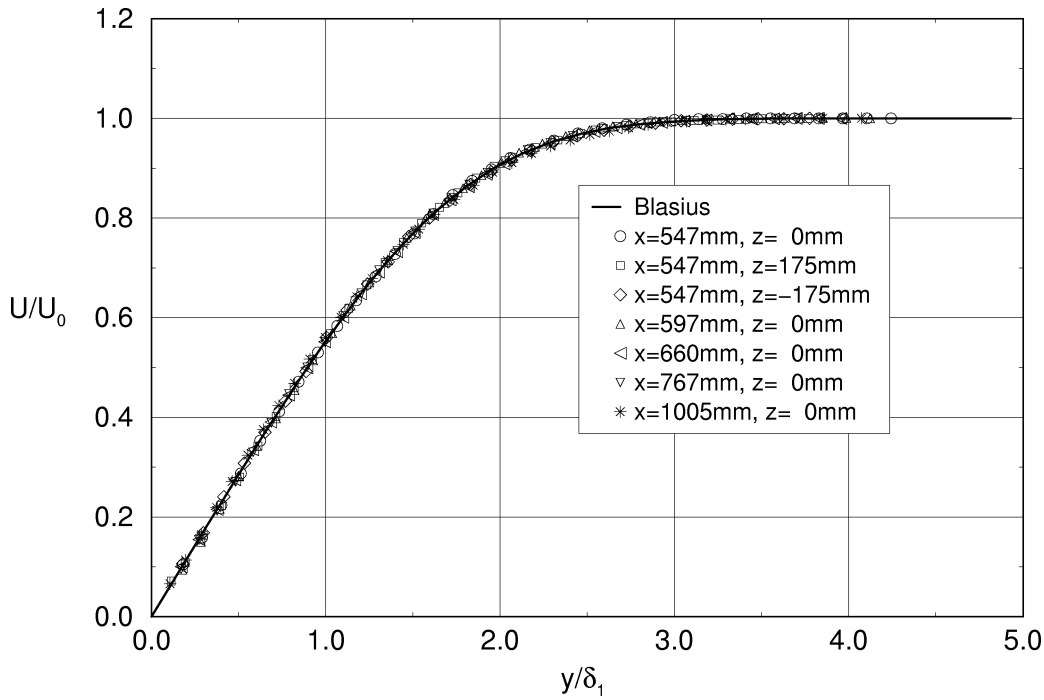

Figure 2. Mean velocity profiles at different streamwise and spanwise positions.

The free-stream velocity U_0 was fixed at 7.2 m/s. At natural disturbance conditions (i.e. without excitation of the instability waves) this velocity corresponds to a Reynolds number $Re = U_0\delta_1/\nu = 763$ at the position of the disturbance source ($x = x_s = 547$ mm) where the boundary layer displacement thickness δ_1 was equal to 1.69 mm. *Figure 2* shows a set of mean-flow velocity distributions $U(y)$ measured in the boundary-layer at 'natural' disturbance conditions at different streamwise and spanwise positions covering the whole range of the coordinates used during the main measurements. These distributions are very close to the Blasius profile (also shown in *figure 2*) despite a presence of a slightly favourable streamwise pressure gradient in the potential flow caused by the growth of the boundary-layer on the test-section wall. Under the conditions of the present experiment the free-stream turbulence level in the test section was below $Tu_\infty = 0.08\%$ in a frequency range between 0.1 and 1000 Hz.

2.2. Generation of disturbances and data acquisition

The experiments were conducted under controlled disturbance conditions. The instability waves were introduced into the boundary layer by means of a novel disturbance source called the 'slit generator'. This generator was designed on a basis of a slit source developed and tested by Gaponenko and Kachanov [42].

A spanwise slit (with width of 0.5 mm, length of 260 mm, and depth of 5.0 mm) was cut into the wall of a special ring-like part of the test section. A set of 32 specially shaped metal pipes (with a spacing of 8 mm each) was positioned under the slit, periodically in spanwise direction. Outside the wind tunnel the pipes were connected to three loudspeakers via 32 plastic tubes. The ring with the slit generator, covering approximately a quarter of the circumference, was inserted between two other sections of the test section and could be rotated in order to change the spanwise position (z-direction) of the source relative to the hot-wire probe mounted on an $x-y$ traverse.

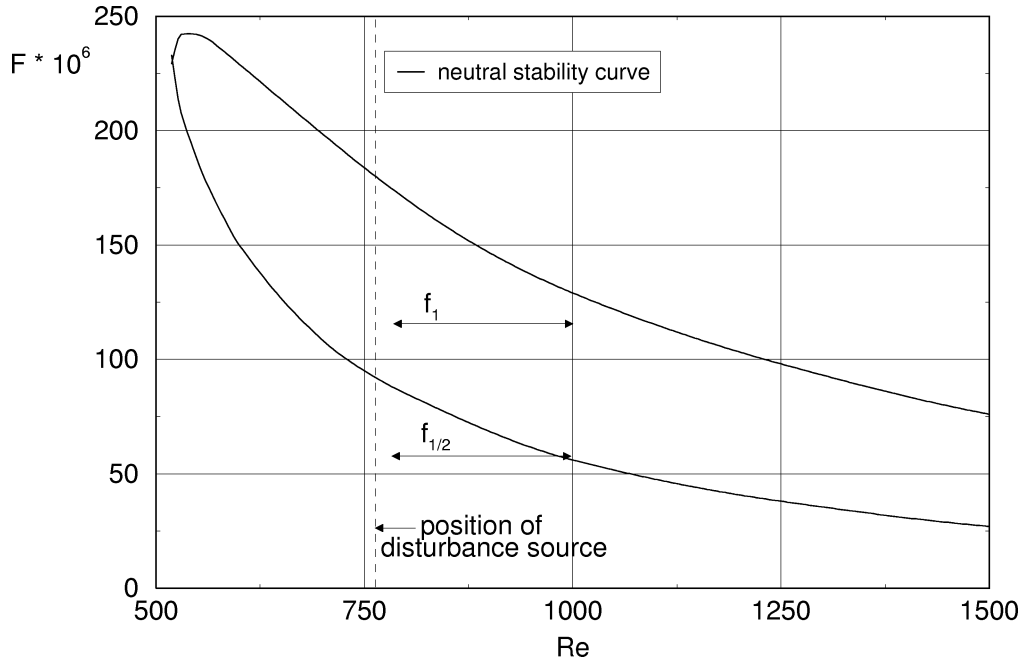

Figure 3. The region of measurements in relation to the neutral stability curve for 2D disturbances in Blasius flow.

In the present experiment it was necessary to excite the boundary-layer with a 2D fundamental wave and/or a pair of 3D oblique subharmonic waves. For this purpose three different time-periodic signals were produced to feed the loudspeakers. The signal generator consisted of a micro-computer, three D/A-converters, and three power amplifiers. Inside the disturbance generator the signals, produced by different loudspeakers, superimpose to form in the flow (near the outlet of the slit) a 2D or 3D disturbance field of volume fluctuations of the fluid.

A constant-temperature hot-wire anemometer with a linearizer was used to measure the streamwise component of the time-mean (U) and fluctuation (u) velocities of the flow. The hot-wire probe (with a wire of 5 μm diameter and 1 mm active length) was mounted on a traverse. The hot-wire signal was sampled and analysed with a Tektronix Fourier analyser. The phase locked ensemble averaged (or instantaneous) time-series, triggered by the excitation signal, were stored in a PC and transfered to a work station for a subsequent analysis. The values of the disturbance amplitudes and phase were determined by means of a Fourier transformation of the time series. Note, that all averaged values of the disturbance amplitudes presented in this paper are determined as r.m.s. values.

2.3. Measurement regimes

The frequency of the fundamental instability wave f_1 excited by the source was chosen as 62.5 Hz and corresponded to a non-dimensional frequency parameter $F = 2\pi f \nu / U_0^2 = 115.5 \times 10^{-6}$. In this case the subharmonic disturbances had the frequency $f_{1/2} = f_1/2 = 31.25$ Hz and a frequency parameter $F_{1/2} = 57.8 \times 10^{-6}$. Shown in *figure 3* is a position of a region of the main measurements for the two spectral modes in the $Re - F$ plane in comparison with the position of the 2D neutral stability curve calculated by Barry and Ross [43] for the Blasius boundary layer. The experimental values of the Reynolds number in this figure were determined using the measured values of the boundary layer displacement thickness in the absence of

the disturbance excitation. Note, that in the beginning of the region of measurements the Blasius flow is even stable with respect to excited two-dimensional subharmonic waves; this is then especially true for the 3D subharmonics.

The values of the subharmonic spanwise wavenumber were conditioned by the spanwise step of the pipes inside the disturbance source ($l = 8$ mm) and were $\beta_{1/2} = \pm 2\pi/\lambda_z = \pm 2\pi/32$ mm$= \pm 0.196$ rad/mm.

Four cases of excitation were investigated:

Case I: Generation of the 2D fundamental instability wave with the amplitude A_1 (large) and the phase φ_1, and a pair of oblique subharmonics with the amplitudes $A_{1/2}$ (low), the phase $\varphi_{1/2}$, and the spanwise wavenumber $\pm\beta_{1/2}$. The phase angle between the fundamental and the subharmonic waves was chosen to be close to a favourable value for the subharmonic resonance following earlier measurements reported by Kachanov and Levchenko [28].

Case II: Generation of a pair of oblique subharmonic waves with the same spanwise wavenumbers $\pm\beta_{1/2}$ and the same low amplitude as in case I.

Case III: Generation of a 2D fundamental wave with the same amplitude as in case I.

Case IV: The same as case I, but with the phase shift between the fundamental and the subharmonic waves orthogonal to the resonant case—an 'anti-resonant' case.

3. Initial stages of disturbance development

3.1. Disturbance field near the source

The 'initial' disturbance conditions were documented in all cases studied at a downstream position close to the disturbance source at $\Delta x = x - x_s = 50$ mm. The perturbations excited in the boundary layer in case I had the following properties. The time-traces obtained at a distance to the wall $y = 1.25$ mm at the spanwise positions $z = -8.0$ and 8.0 mm showed the same shape that is typical for the subharmonic resonance (see for instance Kachanov and Levchenko [28]) with all wave crests at one level but with the valleys oscillating with the subharmonic frequency. These time-traces contain the subharmonic and the fundamental disturbances with the subharmonic wave shifted with respect to the fundamental wave by plus or minus a quarter of its period. Meanwhile, the time-trace obtained at $z = 0$ mm contains only the fundamental wave with the same phase as for $z = \pm 8.0$ mm (this wave is two-dimensional).

The 'initial' spanwise distributions of the disturbance amplitudes and phases are shown in *figure 4*. They were obtained (after Fourier analysis of the time-traces) at $\Delta x = 50$ mm and $y = 0.90$ mm (close to the disturbance amplitude maxima) in the all four cases studied. The fundamental wave demonstrates a nearly two-dimensional behaviour with regard to its amplitude and phase (*figures 4(a)* and *4(b)*). The resonant case I and the anti-resonant case IV differ by a shift of the fundamental wave phase by 180° (*figure 4 (b)*). The distributions of the subharmonic amplitude and phase shown over one spanwise period in *figures 4(c)* and *4(d)* display a shape which results from a superposition of two oblique waves with the spanwise wavenumbers $+\beta_{1/2}$ and $-\beta_{1/2}$.

The normal-to-wall profiles of the disturbance amplitude and phase obtained in the 'initial' downstream position at $z = -8.0$ mm are shown in *figure 5* for all four cases studied. The y-coordinate is shown in *figure 5* in 'mm'; the local boundary layer displacement thickness was $\delta_1 = 1.74$ mm. The fundamental wave profiles (*figures 5(a)* and *5(b)*) have shapes which are typical for 2D Tollmien–Schlichting waves, whereas the subharmonics have profiles (*figures 5(c)* and *5(d)*) characteristic of 3D instability waves in the Blasius flow.

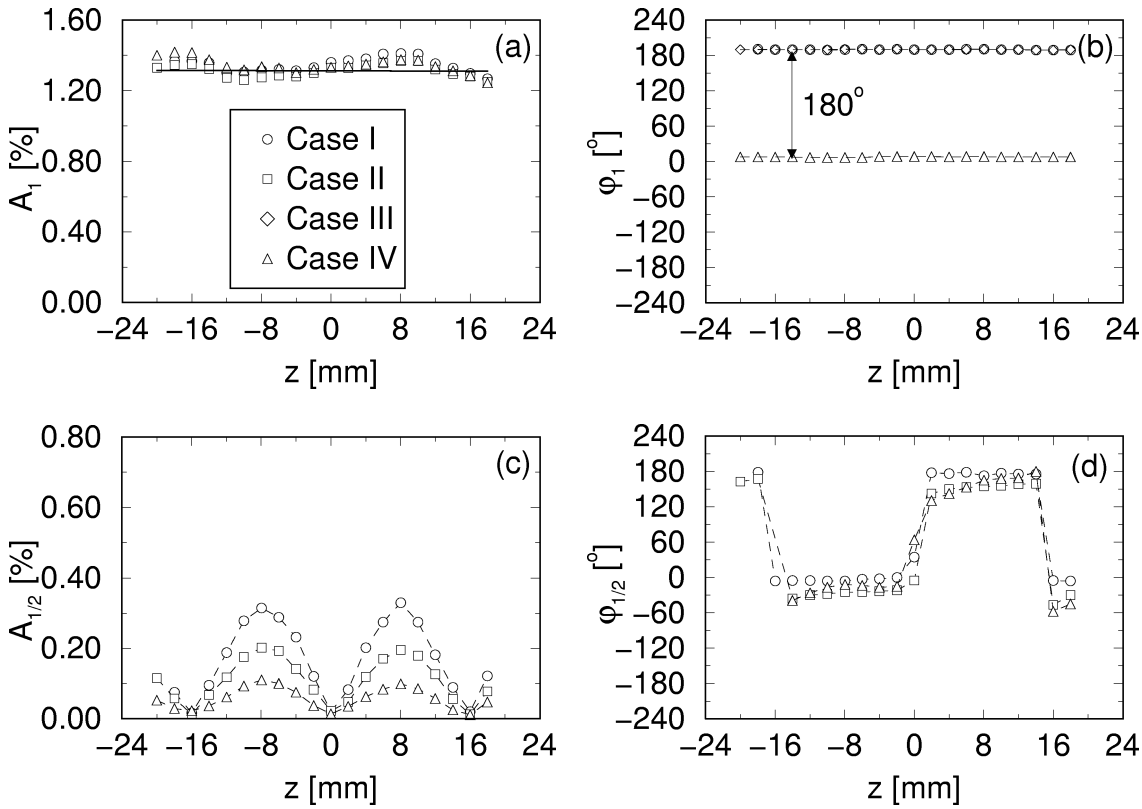

Figure 4. 'Initial' spanwise disturbance profiles measured at $\Delta x = 50$ mm and $y = 0.90$ mm for all four cases. Fundamental wave: (a) amplitude, (b) phase. Subharmonic wave: (c) amplitude, (d) phase.

All main properties of the 'initial' instability modes generated in the flow in all four cases are typical of those of the linear instability modes. However, the effect of the subharmonic resonance (case I) and the anti-resonance (case IV) can already be seen at $\Delta x = 50$ mm downstream the source. A significant difference in the subharmonic amplitudes is observed in cases I, II, and IV (*figures 4(c)* and *5(c)*). *Figures 4* and *5* show also that in the present experiment the 'initial' amplitudes of the fundamental wave were about 1.3% in all cases when it was excited, while the 'initial' amplitudes of the two oblique subharmonics were around 0.15% only. (After 'in-phase' superposition of these two modes the total maximum intensity of the disturbance at the subharmonic frequency is equal to about 0.3%.)

3.2. Downstream evolution of the instability waves

The downstream development of the instability waves (shown in *figure 6*) was studied at a spanwise position where the subharmonic amplitudes had their maximum ($z = -8.0$ mm) and at a constant non-dimensional distance to the wall $y/\delta_1 = 0.52$ where the amplitudes of all three waves were close to their maximum in the y-profiles. (Note that the measurements of the normal-to-wall disturbance profiles conducted at the last streamwise position of the initial region (at $\Delta x = 220$ mm) showed that the shape of the profiles remained qualitatively the same as at the 'initial' position (see *figure 5*).)

Figure 6(a) shows that the fundamental amplitude is almost completely independent of the four cases and depends only weakly on the streamwise coordinate. This means that in the initial region, discussed in the

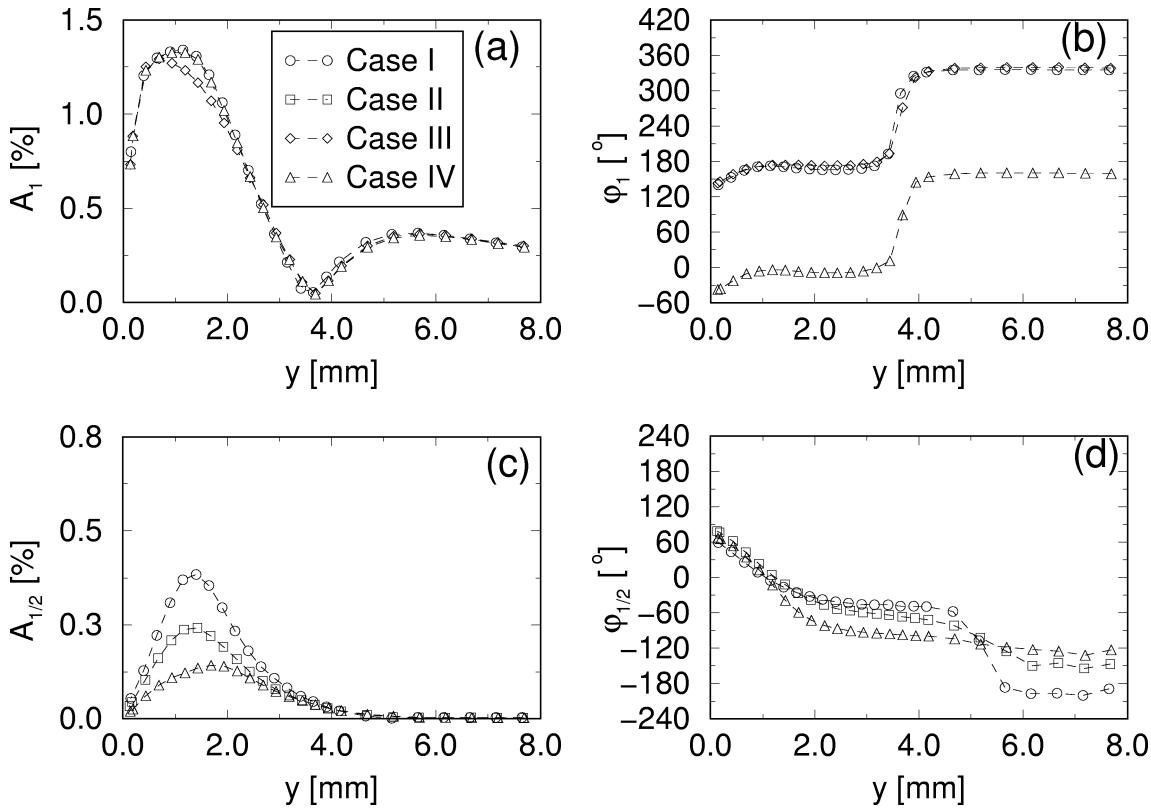

Figure 5. 'Initial' normal-to-wall disturbance profiles measured at $\Delta x = 50$ mm and the peak position ($z = -8$ mm). Fundamental wave: (a) amplitude, b) phase. Subharmonic wave: (c) amplitude, (d) phase.

present section, the fundamental wave is not influenced by an interaction with the subharmonic wave and plays a 'catalytic' role in the subharmonic resonance observed in case I (e.g. Herbert [21], Kachanov [25]); i.e. the interaction remains parametric in this region. This property is rather typical for the subharmonic resonant interactions in the boundary layer although the back influence of the subharmonics on the fundamental mode can be important even at rather low subharmonic amplitudes (around 1%) when the fundamental amplitude is also small, even smaller than the subharmonic one (see Corke and Mangano [29]).

In contrast to the fundamental disturbance the behaviour of the subharmonic amplitudes is significantly different in the three cases studied (*figure 6(b)*). In case II (excitation of the subharmonics only) the subharmonic amplitude decreases downstream, in consistence with linear stability theory (see *figure 3*), with a rate $-\alpha_{i1/2} = -5.43 \cdot 10^{-3}$ mm^{-1}. Whereas in case I a rapid exponential growth with a rate $-\alpha_{i1/2} = 1.1 \times 10^{-2}$ mm^{-1} is observed. This behaviour is in a qualitative agreement with the linear Floquet theory Herbert [4] and with the weakly-nonlinear theory (see Craik [18] and Volodin and Zelman [36]). Both theories predict an exponential growth of the subharmonic amplitude when the fundamental amplitude remains constant (*figure 6(a)*). In the anti-resonant case IV, when the initial phase shift between the fundamental and the subharmonic wave is orthogonal to the resonant case I, the amplitude of the subharmonic attenuates initially faster than in the 'linear' case II. Further downstream the subharmonic amplitude grows slightly again, probably because of the amplification of a very small but remaining resonant component of the subharmonics.

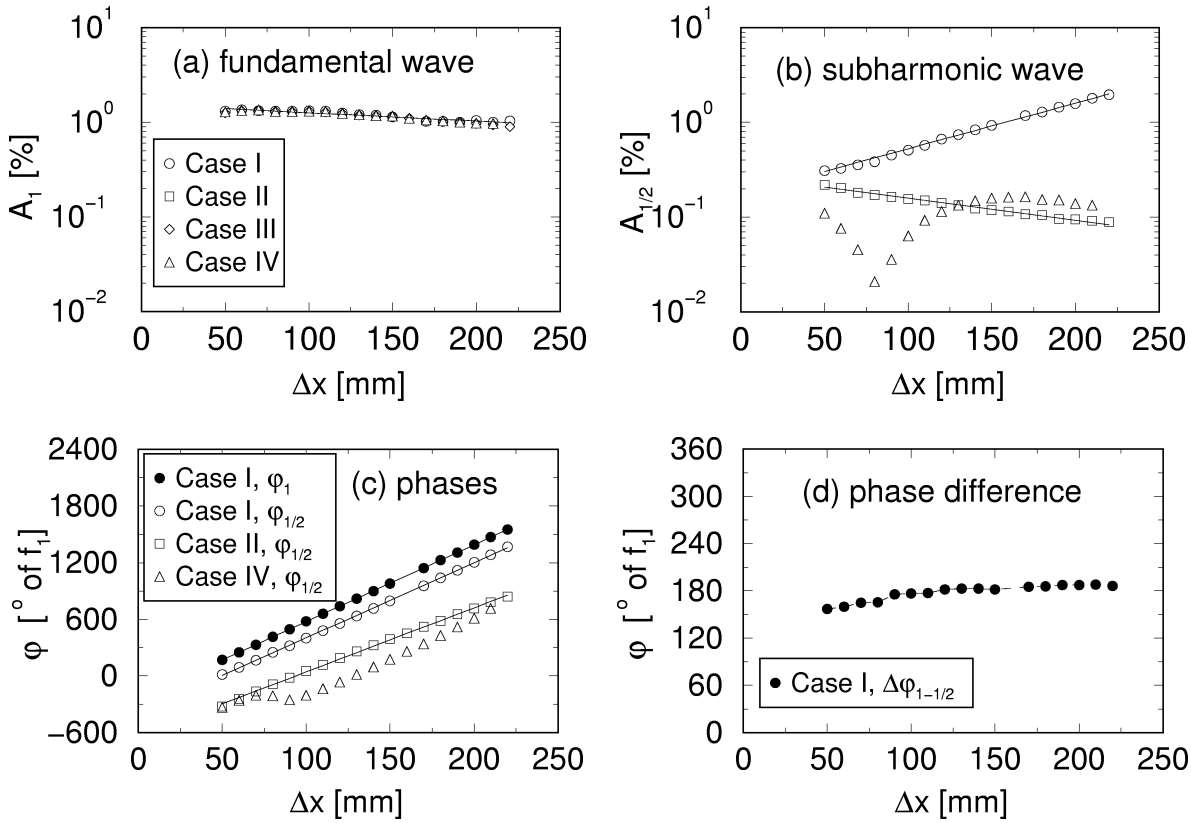

Figure 6. Streamwise development of the instability waves at the spanwise peak position ($z = -8$ mm) and at $y/\delta_1 = 0.52$. (a), (b) amplitudes; (c) phases; (d) phase difference.

The phase synchronisation of the interacting modes is the main condition necessary for the existence of the three-wave resonant interaction between the modes, in particular for the parametric subharmonic resonant interaction (see Craik [18], Herbert [4]). These conditions are

$$\omega_1 = \omega_{1/2} + \omega_{1/2},$$
$$\alpha_1 = \alpha_{1/2} + \alpha_{1/2},$$
$$\beta_1 = \beta_{1/2} + (-\beta_{1/2}),$$

giving an equality

$$\frac{\omega_1}{\alpha_1} = \frac{\omega_{1/2}}{\alpha_{1/2}} \quad \text{or} \quad C_{x1} = C_{x1/2},$$

where $\omega_1 = 2\pi f_1,\ \omega_{1/2} = 2\pi f_{1/2},\ C_{x1}$ and $C_{x1/2}$ are the downstream phase velocities and α_{r1} and $\alpha_{r1/2}$ are the streamwise wavenumbers of the fundamental and subharmonic instability modes, respectively.

The phase velocities and the other dispersion characteristics of the disturbances were determined in the present experiments (*table I*) by means of a least square fit with straight lines (see *figure 6(c)*). It is seen from *table I* that in case II (the subharmonics only) the subharmonic phase speed is about 20% higher than that of the fundamental wave in case I. This is due to the fact that the subharmonic waves have a somewhat greater spanwise wavenumber $\beta_{1/2}$ than is necessary for exact satisfaction of the resonant condition and, consequently, somewhat higher propagation angle $\omega_{1/2}$. Meanwhile in case I the resonant interaction provides an additional

Table I. Dispersion characteristics of instability waves at initial stage of development.

	$\beta_{1/2}$ [rad/mm]	$\lambda_{z1/2}$ [mm]	α_{r1} [rad/mm]	$\alpha_{r1/2}$ [rad/mm]	λ_{x1} [mm]	$\lambda_{x1/2}$ [mm]	C_{x1}/U_∞	$C_{x1/2}/U_\infty$	Θ_1 [°]	Θ_1 [°]
Case I	±0.196	32.0	0.142	0.0693	44.38	90.64	0.385	0.394	0.0	±70.6
Case II	±0.196	32.0	—	0.0591	—	106.38	—	0.461	—	±73.2
Case III	—	—	0.142	—	44.17	—	0.384	—	0.0	—

synchronisation of the instability modes amplifying only the resonant component of the subharmonic wave which has a phase favourable for the resonance (see e.g. Kachanov [25]). Due to this the synchronism condition is satisfied in case I almost perfectly and the phase speeds of the fundamental and subharmonic waves differ only by 2%.

We can conclude that the behaviour of the disturbances in case I is typical of the initial stages of the N-regime of transition described in the introduction (sub-regime (ii) with regular subharmonic perturbations). The transition process observed in case I is dramatically different from that observed in cases II–IV although the 'only' difference between case I and case IV is the phase shift of the fundamental wave by 180°! In case I the transition develops very rapidly due to the resonant interaction of the instability waves leading to the formation of Λ-structures (see the next section) and the final breakdown of the flow. In the other regimes the growth of the perturbations is either much weaker or was not observed at all (as in case II).

According to the main goal of the present study, we concentrate below on the development of the transition process in case I, in order to clarify the physical mechanisms of the late stages of the N-regime of breakdown.

4. Formation of Λ-structures and spikes

The structure of the disturbance field (case I) was studied in detail downstream of the initial stage. The measurements discussed mainly in this section were performed at $\Delta x = 380$ mm where the hot-wire was traversed to $17 \times 38 = 646$ positions in a (y, z)-plane perpendicular to the mean-flow direction. Phase-locked ensemble averaged time-series were sampled and stored in the computer. In this way the periodical part of the instantaneous flow field passing through the plane of measurement was reconstructed. Note, that despite the high magnitude of perturbations the transitional flow was mainly periodical at $\Delta x = 380$ mm and the intensity of the random fluctuations was still rather low.

4.1. Formation of peaks and valleys

The formation of peaks and valleys of the N-regime of transition was observed already upstream of $\Delta x = 380$ mm and is therefore illustrated at $\Delta x = 220$ mm.

Figure 7 shows the spanwise distributions of the disturbance amplitudes and phases for the main spectral modes. The total intensity u' of the disturbances becomes strongly modulated along the span similar to the amplitude of the subharmonic wave that already dominates the flow. The subharmonic amplitude $A_{1/2}$ reaches rather high values here (about 2.1% in the peak position) which are much larger than those in the 'initial' position (about 0.3% in the peak position). The subharmonic amplitude is also significantly greater than the amplitude of the fundamental wave A which still remains quasi two-dimensional and has an amplitude of about 1% which is even lower than in the 'initial' position (1.3%).

The jumps observed in the subharmonic phase distribution show that the two peak positions in *figure 7* are split in time and, consequently, in the x-direction. This feature of the present stage of the N-breakdown is

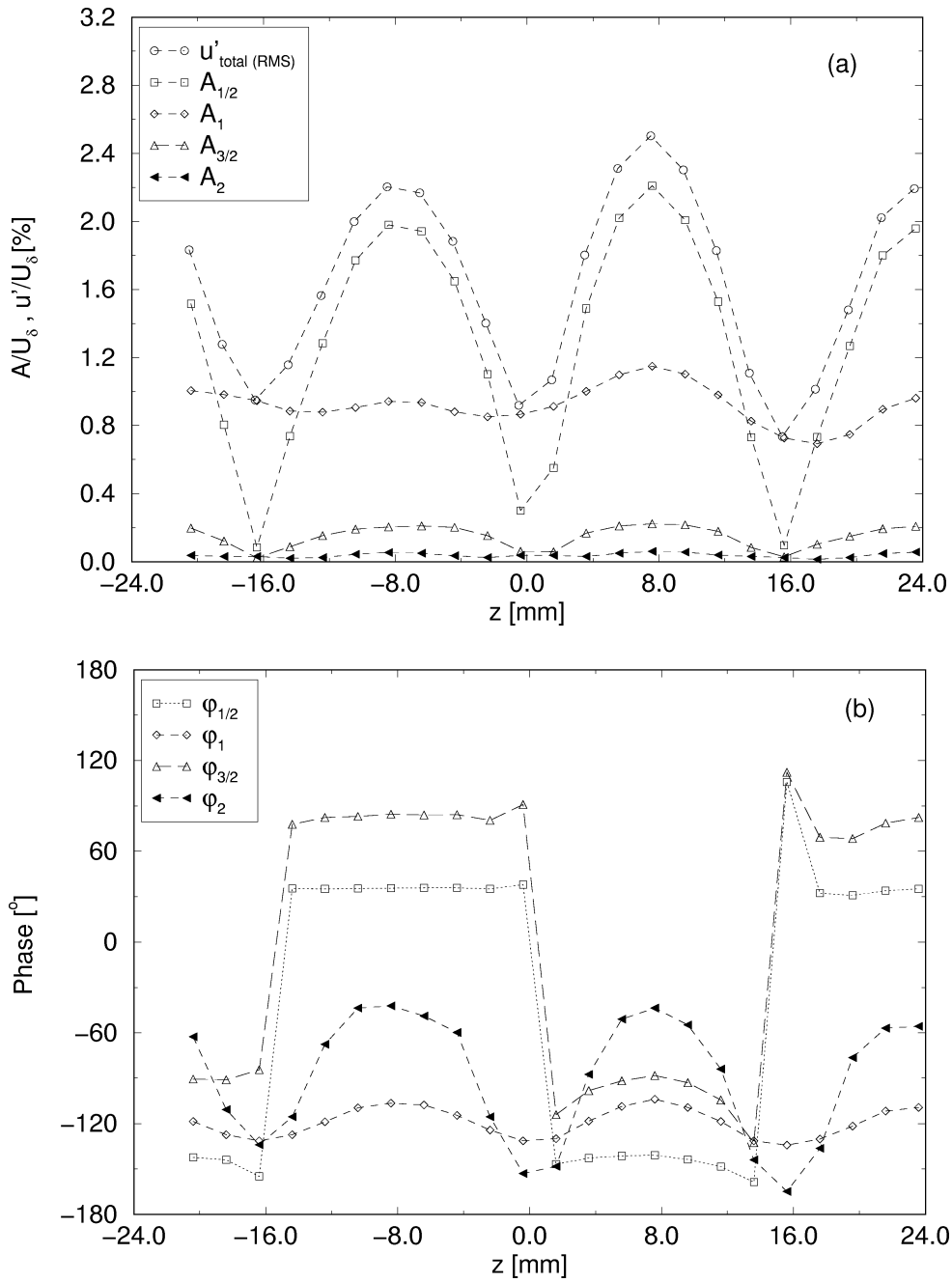

Figure 7. Spanwise distributions of the disturbance amplitudes (a) and the phases (b) at $\Delta x = 220$ mm, $y = 1.36$ mm. Case I.

different from the corresponding stage of the K-regime where the dominating mode is the fundamental wave and its phase has the same value at different peak positions (see e.g. Kachanov et al. [10]).

A spanwise Fourier decomposition of the distributions presented in *figure 7* has shown that the pair of 3D subharmonics excited by the source (with $\beta_{1/2} = \pm 0.196$ rad/mm) dominates already in the flow and they

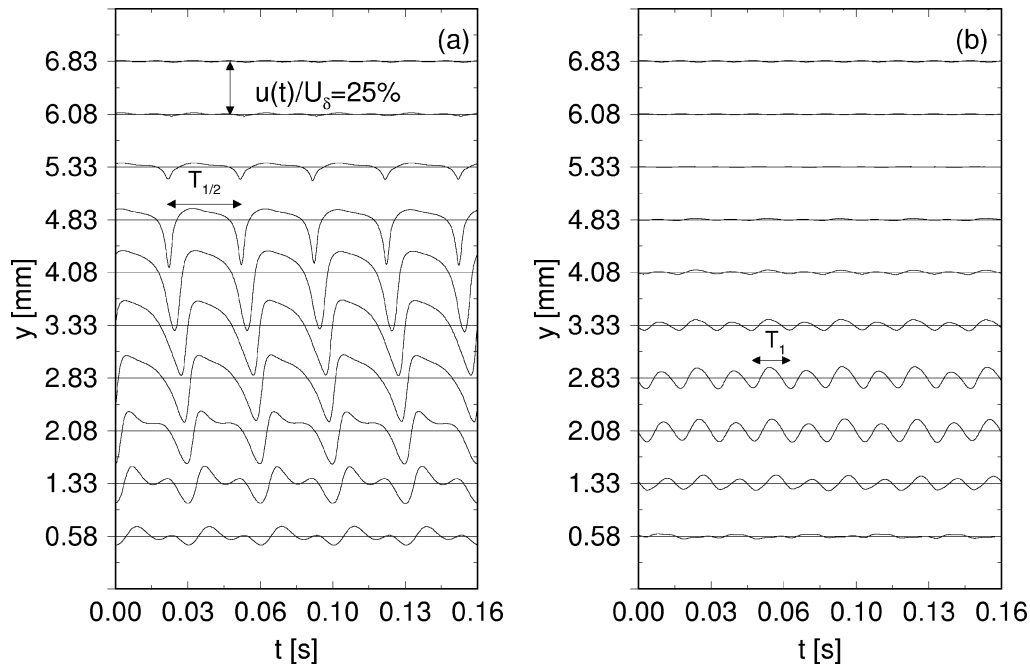

Figure 8. Ensemble averaged time-traces obtained at $\Delta x = 380$ mm at two spanwise position and various distances above the wall. (a) peak: $z = -8$ mm; (b) valley: $z = 0$ mm. Case I.

remain the most intensive modes in the subharmonic spanwise-wavenumber spectrum. At the fundamental frequency the 2D mode still dominates despite its attenuation and its 3D components remain relatively small.

4.2. Time-traces and frequency spectra

Figure 8 shows two sets of ensemble-averaged time-traces obtained at Δx = 380 mm in the peak ($u'(z) =$ max, $z = -8.0$ mm) and valley ($u'(z) = \min$, $z = 0$) positions for different distances y from the wall. The local boundary-layer thickness $\delta_{99.5\%}$ was equal to 6.92 mm in the peak position and 6.66 mm in the valley position. The peak position shows clearly the beginning of the process of spike formation, typical of the breakdown of the K-regime (see e.g. Borodulin and Kachanov [17]). The spikes have a characteristic shape, very high amplitude (more then 35%), and develop in the outer part of the boundary layer (at $y/\delta \approx 0.6$). In the valley position the amplitude of the disturbances is very low, the shape of the time-traces remains almost sinusoidal and keeps the fundamental wave periodicity with the period $T_1 = 1/f_1 = 0.016$ s. In contrast to the K-regime the spikes appear with the subharmonic time period $T_{1/2} = 1/f_{1/2} = 0.032$ s.

The shape of the 'early' spikes seen in the time-trace, presented in *figure 8* at $y = 4.08$ mm ($y/\delta = 0.6$), can be characterised by its frequency spectrum which is plotted in logarithmic scale in *figure 9*. In agreement with previous observations of the K-regime (see Borodulin and Kachanov [13,17] and Kachanov et al. [24]) the amplitudes of the spectral harmonics attenuate with frequency according to a geometric progression (i.e. exponentially) that corresponds to a straight-line envelope. At the initial stages of formation of spikes in the K-regime (Borodulin and Kachanov [17]) the geometric progression factor q increases very rapidly with x from 0.4 to 0.9 and can play a role as a quantitative measure of the stage of the spike formation. In the present case the factor q is 0.54 characterising a relatively early stage of spike formation at position $\Delta x = 380$ mm.

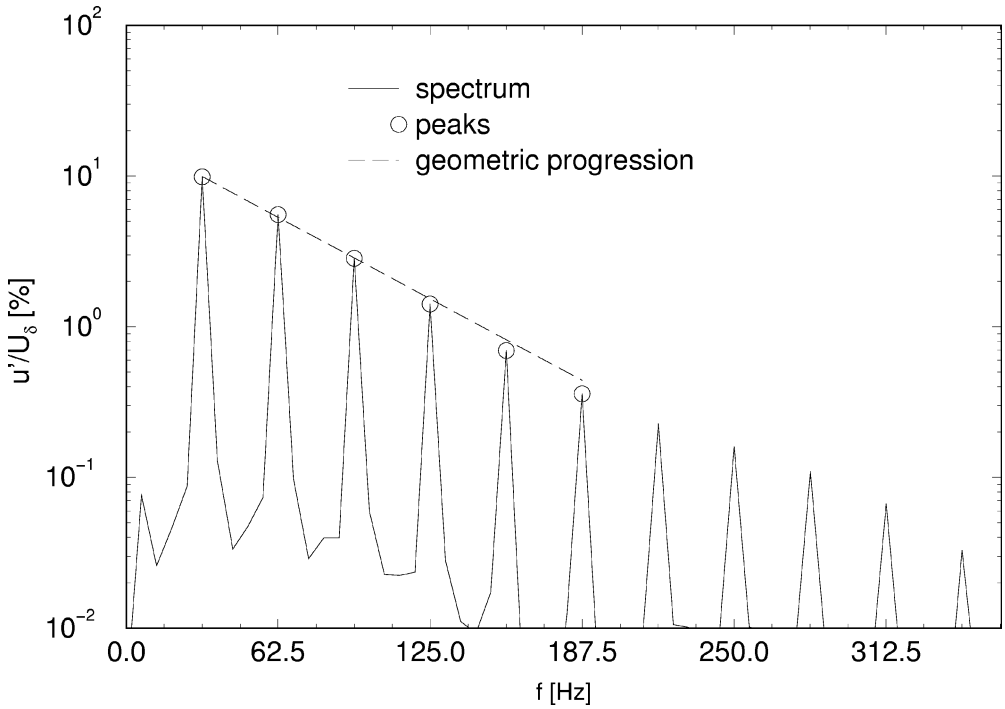

Figure 9. Frequency spectrum of time-traces with spikes at $\Delta x = 380$ mm, $y = 4.08$ mm, $z = -8.0$ mm (peak). Case I.

4.3. Instantaneous velocity distributions

The formation of the Λ-structures in a staggered order can be seen in contour plot distributions of the instantaneous streamwise velocity disturbance u/U_0 in the $(-t, z)$-plane shown in *figure 10* for Δx = 380 mm and several fixed distances above the wall $y = 4.08,\ 3.33,\ 2.58$ and 0.58 mm. Far from the wall (*figure 10(a)*) the regions with an intensive negative fluctuation of the instantaneous streamwise velocity are located at the peak positions and correspond to the tip of the Λ-structure and the location of an 'early' spike. Closer to the wall (*figures 10(b)* and *10(c)*) the shape of the Λ-structure nose is seen at later time moments or, what is the same, upstream from the tip. Near the wall (*figure 10(d)*) each of the low speed regions is divided in the spanwise direction into two regions which correspond to the 'legs' of the Λ-structure.

The Λ-shaped character of the instantaneous-velocity structures is seen in a 'projection' of the instantaneous streamwise velocity field (again in $(-t, z)$-plane) onto the surface of the model (*figure 11*). This 'projection' was obtained by an integration of the instantaneous velocity disturbance in y-direction according to the formula

$$\tilde{u}(t, z)/U_0 = 1/\delta \int_0^\delta u(t, y, z)/U_0 \, dy.$$

Figure 12 shows three sets of instantaneous profiles of the streamwise velocity $\widehat{U}/U_0 = U/U_0 + u/U_0$ obtained at $\Delta x = 380$ mm at three spanwise positions (peak, valley, and another peak). Similar to the K-regime of breakdown (see Kovasznay et al. [7] and Borodulin and Kachanov [17]) the profiles demonstrate the formation of a high-shear layer with high values of the total spanwise vorticity $\widehat{\Omega}_z = \Omega_z + \omega_z$ which almost coincide in boundary layers with the shear $\partial\widehat{U}/\partial y = \partial U/\partial y + \partial u/\partial y$. In the N-regime the regions of high spanwise

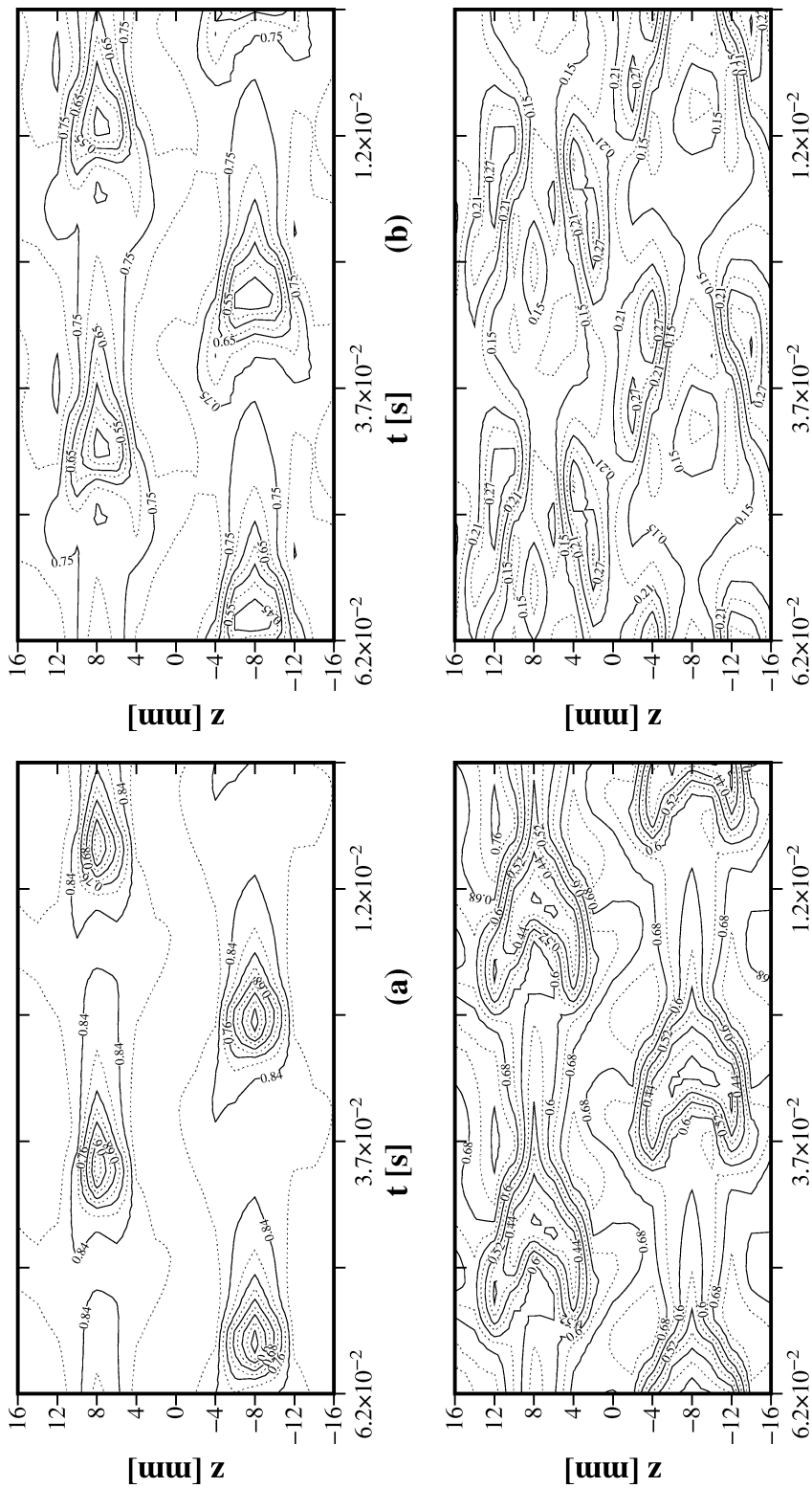

Figure 10. Contours of instantaneous streamwise velocity disturbance in $(-t, z)$-planes measured at $\Delta x = 380$ mm and (a) $y = 4.08$ mm; (b) $y = 3.33$ mm; (c) $y = 2.58$ mm; (d) $y = 0.58$ mm. Case I.

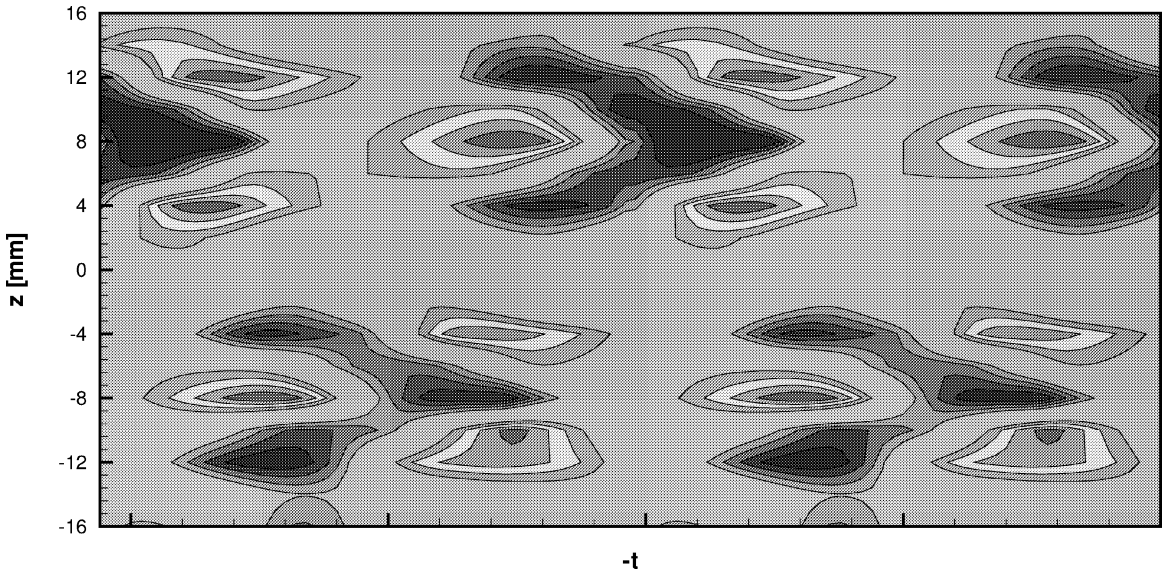

Figure 11. 'Projection' $\tilde{u}(t,z)/U_0$ of instantaneous distributions of fluctuating streamwise velocity onto the wall in the $(-t,z)$-plane obtained at Δx = 380 mm, shown for two subharmonic periods in time and one subharmonic spanwise period in space. Case I.

vorticity have subharmonic periodicity (both in span and in time) and are positioned in space in the staggered order. The spatial shape of the spanwise vorticity field is discussed in more detail in the next subsection.

4.4. Fields of instantaneous spanwise vorticity

The fields of the mean vorticity Ω_z, the instantaneous vorticity disturbance ω_z, and the instantaneous total vorticity $\widehat{\Omega}_z = \Omega_z + \omega_z$ were determined from the measured ensemble-averaged velocity field as: $\Omega_z = \partial U/\partial y,\ \omega_z = \partial u/\partial y$. The spanwise vorticity concentrations show the shape of the high-shear layers. Similar to the instantaneous-velocity structures (see *figures 10* and *11*) the high-shear layers are also Λ-shaped. However, the latter are displaced somewhat further from the wall than the former. This fact agrees with the DNS results obtained by Rist and Fasel [26] for the K-regime of breakdown, as well as their inclined position of the structures to the wall. The Λ-shaped form of the high-shear layers in plan view maybe seen from a 'projection' of the 3D picture (not shown) that looks very similar to the picture obtained by Kovasznay et al. [7] in the K-regime and called 'Δ-wing shaped' high-shear layer.

A detailed information about the instantaneous spanwise vorticity field can be obtained from sections of the spatial picture by the $(-t, y)$- and (y, z)-planes at various fixed z- and t-coordinates, respectively. *Figure 13(a)* shows contours of constant values of the instantaneous total spanwise vorticity $\widehat{\Omega}_z$ obtained at two peak positions ($z = -8.0$ and $+8.0$ mm). Very similar pictures were obtained in the K-regime of breakdown in experiments by Kovasznay et al. [7], in the DNS of Kleiser and Zang [23] and in experiments by Borodulin and Kachanov [17] for approximately the same stage of the disturbance development corresponding to the appearance of the first spike. The only difference again is the order of the structures and the period of their appearance.

Isolines of the instantaneous spanwise vorticity Ω_z are plotted in (y, z)-planes at several time instants (within one subharmonic period) in *figure 14*. This picture shows the normal-to-wall structure of the vorticity field. The region of high shear located in the tip of the Λ-structure splits with time into two regions (the Λ-structure 'legs') which move away from the peak position towards the wall. Under the high-shear layers with positive

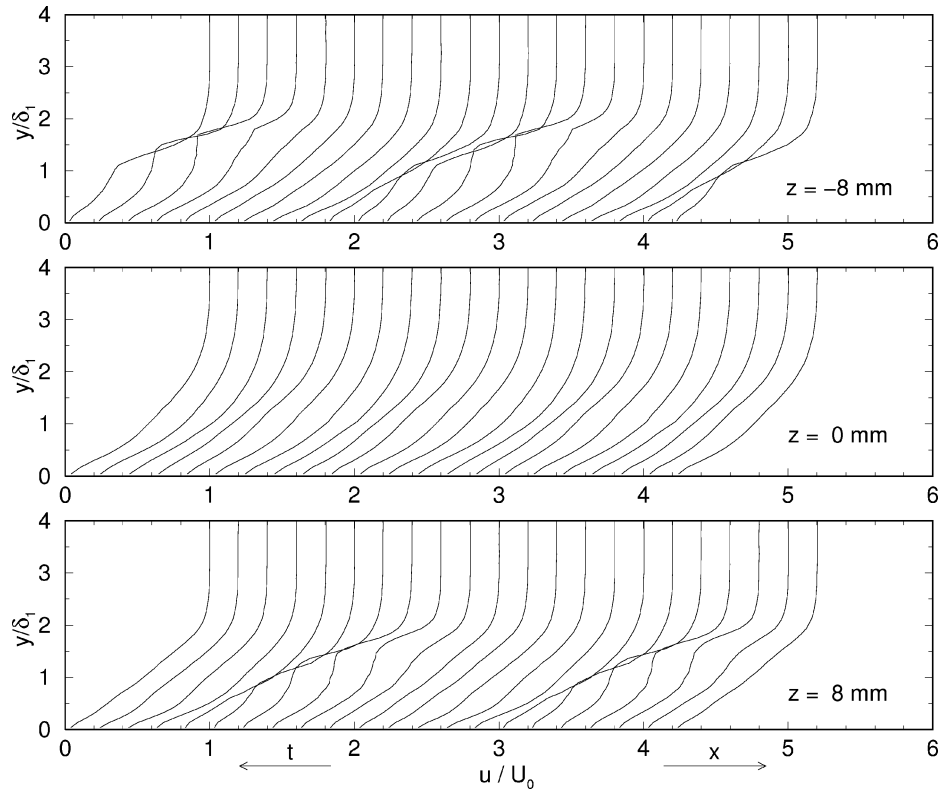

Figure 12. Instantaneous profiles of total streamwise velocity obtained at $\Delta x = 380$ mm at three spanwise positions (peak, valley, peak). Case I. The profiles are displaced along the horizontal axis with a constant step.

values of spanwise vorticity there are regions with high negative shear. These regions show a similar behaviour in time but remain separated in the spanwise direction and do not merge near the Λ-structure tip. This structure of the vorticity field in the vicinity of the Λ-vortex is qualitatively exactly the same as that found in DNS for the K-regime of the boundary layer breakdown (Rist [22]). The only difference with the present case (N-regime) is the order of the structures in (x, z)-plane and their time periodicity.

4.5. Subsequent behaviour of perturbations

The analysis of the experimental data obtained at the streamwise positions $\Delta x = 50$ to 380 mm gives us two main results. First, the regime of transition observed in case I has all attributes of the initial stages of the N-regime of the boundary-layer breakdown which are well known from previous experimental and theoretical studies. In particular, the beginning of the transition is conditioned by the resonant growth of the 3D subharmonic waves and characterised by the formation of the Λ-structures in staggered order. Secondly, the local disturbance field in the vicinity of the Λ-structure at the stage $\Delta x = 380$ mm turned out to be qualitatively similar to the K-regime of breakdown. At this stage the Λ-structures are fully developed (not 'primary' ones) and have high concentrations of vorticity in the Λ-structure 'legs' and 'tip' and a strongly developed 3D high-shear layer (also Λ-shaped) with all characteristics typically observed in the K-regime of breakdown. Finally, the streamwise position $\Delta x = 380$ mm of the present N-regime is characterised by an initial stage of formation of the spikes which has been observed before only in the K-regime. All properties of these spikes, their spatial position, shape, and special spectral characteristics, are typical of the spikes studied in the K-regime.

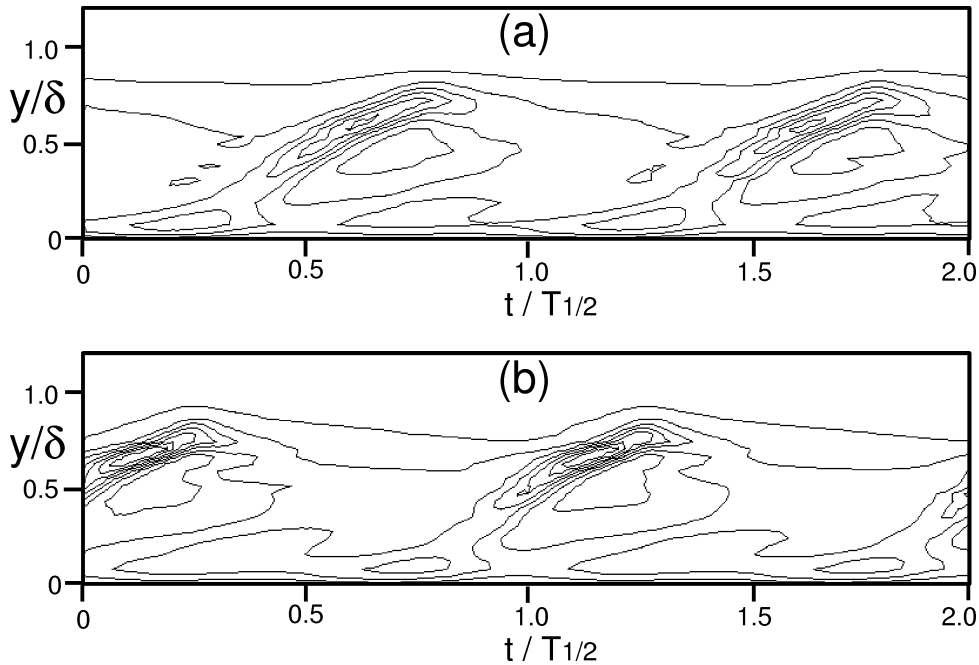

Figure 13. Contours of total instantaneous spanwise vorticity Ω_z at peak position $\Delta x = 380$ mm, case I); (a) $z = -8.0$ mm, (b) $z = 8.0$ mm.

The subsequent development of the spikes in the N-regime of transition (case I) is illustrated in *figures 15(a)–15(c)* by three sets of time-traces (not ensemble-averaged), measured at three streamwise positions ($\Delta x = 420,\ 440$, and 460 mm) on the peak position line ($z = -8.0$ mm) at various distances above the wall. The first spike becomes very sharp at Δx = 420 mm and moves towards the edge of the boundary layer ($y/\delta \approx 1$). Further downstream it becomes even sharper and its normal position remains nearly constant. At Δx = 440 and 460 mm the second, third and fourth spikes also appear within each subharmonic period and also have a sharp shape. The greater the number of the spike the closer to the wall they develop; nevertheless all spikes are positioned finally in the external part of the boundary layer.

This behaviour of perturbations is qualitatively the same as observed in the K-regime of the boundary-layer breakdown. The doubling tripling, etc. of the spikes was observed in the K-regime in many experiments (starting with Klebanoff et al. [1] and in numerical simulation (e.g. Rist and Kachanov [27]). The movement of the spikes toward the boundary-layer edge and their specific position relative to the wall shown in *figure 15* were also observed in the K-regime in experiments by Kachanov et al. [10], Borodulin and Kachanov [14,17] and in DNS of Rist [22], Rist and Kachanov [27] and others.

A detailed comparison of the time-traces (N-regime) with those measured in the K-regime in experiment (Borodulin and Kachanov [14,17]) can be made with *figure 15(d)*. This figure shows a set of time-traces measured in the K-regime at the peak position at a stage of the disturbance development close to that illustrated in *figures 15(a)–15(c)*. It is seen that *figures 15(c)* and *15(d)* look qualitatively the same (especially with respect to the spikes). Even some very peculiar details do coincide. For instance, above and below the spikes some small-amplitude 'positive' spikes are observed in the two cases. Their position in time coincides with the position of the large negative spikes. These positive spikes are discussed in Kachanov [12], Borodulin and Kachanov [17] and corresponds to a positive velocity fluctuation around the external edge of the ring-like vortex (the *CS*-soliton) attributed to the spike at late stages of the K-regime of transition. Observation of similar

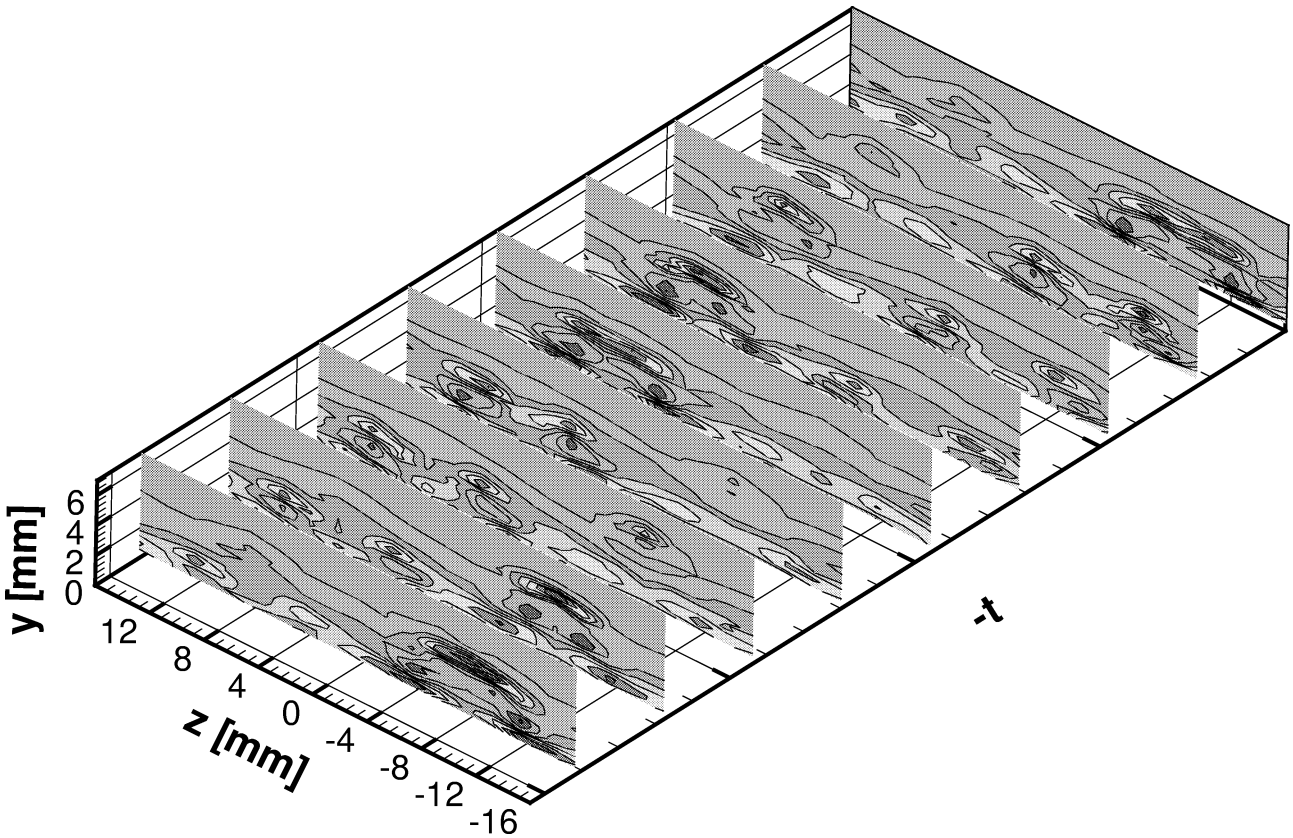

Figure 14. Contours of instantaneous spanwise vorticity Ω_z measured for several time moments within one subharmonic period at $\Delta x = 380$ mm. Case I.

small-amplitude positive spikes around each of the large-amplitude negative spikes in the present study suggests that the soliton-like structures (the ring-like vortices) are also formed at late stages of the N-regime of transition.

The only significant difference between *figures 15(a)–15(c)* and *15(d)* is the time periodicity of the groups of spikes—the subharmonic period in the present experiments (the N-regime) and the fundamental period in experiment Borodulin and Kachanov [17] (the K-regime). Of course, the spatial order of the groups of spikes is also different in these two regimes—staggered in the present case (see *figure 16*) and aligned-in-rows in the K-regime.

5. Conclusions

In the present paper the N-regime of boundary layer transition was generated under controlled disturbance conditions by means of excitation of a 2D fundamental wave with initial amplitude about 1.3% and a pair of 3D subharmonics with initial amplitudes about 0.15%. It is shown that the instability modes having been introduced separately are stable or close to neutrally stable ones and the transition (the N-regime) only occurs when the phase synchronism conditions for subharmonic resonance are satisfied and the phase shift between the fundamental wave and the pair of oblique subharmonics is favourable for this resonance. In this case detailed hot-wire measurements have shown the formation of 'primary' Λ-structures positioned in staggered order with the subharmonic frequency as it was observed in previous studies of the N-regime.

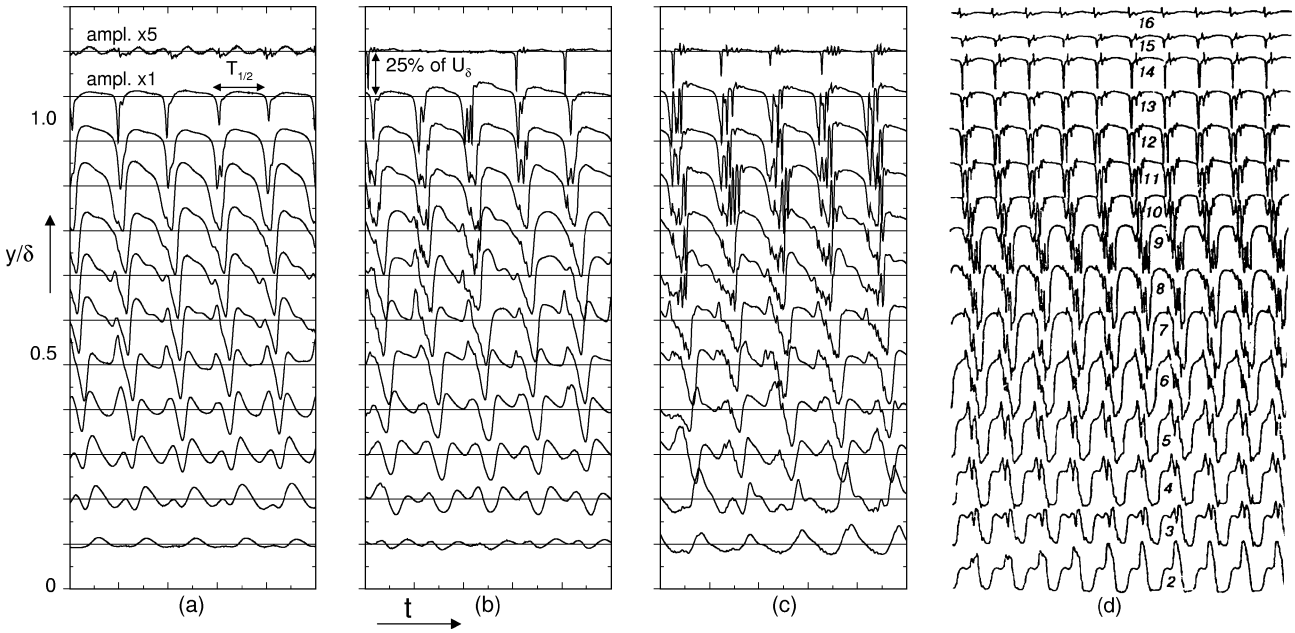

Figure 15. Time-traces obtained far from the source at three consecutive streamwise positions and various distances from the wall in the peak position ($z = -8.0$ mm). Case I. (a)–(c) $\Delta x = 420,\ 440$, and 460 mm, respectively. (d) Time-traces obtained by Borodulin and Kachanov [17] in the K-regime of transition at $\Delta x = 500$ mm and at various distances above the wall in the peak position.

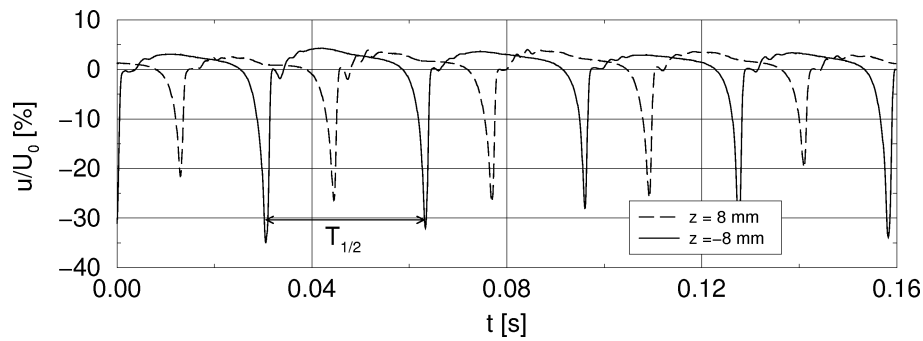

Figure 16. Time-traces obtained at two different peak positions at $\Delta x = 410$ mm, $y = 6.0$ mm, $z = \pm 8.0$ mm. Case I.

The downstream development of the N-regime of transition is found to be qualitatively the same as observed in the 'other' well-known (and carefully studied) regime of breakdown called the K-regime and shows the following features:

(a) growth of the spanwise modulation of the disturbance amplitude and formation of peaks and valleys,
(b) formation of very intensive Λ-structures with a very strong vorticity concentration in its 'legs' and 'tip',
(c) formation of Λ-shaped (or Δ-wing-shaped) 3D high-shear layers,
(d) the appearance of a first, second, third, etc. spike in the peak position near the Λ-structure tip, and
(e) further downstream the formation of ring-like vortices (associated with the spikes) which are snatching away from the Λ-vortex, moving upward, accelerating, and propagating downstream in the external part of the boundary layer.

These results testify that at late stages of the N-breakdown the local physical mechanisms of the nonlinear disturbance development are qualitatively the same as those characteristic of K-regime transition. Consequently, a ‘convergence’ of the mechanisms of the N- and K-breakdown is observed at late stages of the laminar-turbulent transition showing of a qualitative similarity of the local processes of nonlinear disturbance development in the vicinity of the Λ-structure.

References

[1] Klebanoff P., Tidstrom K., Sargent L., The three-dimensional nature of boundary-layer transition, J. Fluid Mech. 12 (1962) 1–34.
[2] Kachanov Y., Kozlov V., Levchenko V., Nonlinear developement of a wave in a boundary layer, Izv. Akad. Nauk SSSR, Mekh. Zhidk. Gaza 5 (1977) 85–94 (in Russian). Transl. Fluid. Dyn. 12 (1978) 383–390.
[3] Zelman M., Maslennikova I., Tollmien–Schlichting-wave resonant mechanism for subharmonic-type transition, J. Fluid Mech. 252 (1993) 499–578.
[4] Herbert T., Analysis of the subharmonic route to transition in boundary-layers, AIAA Paper No. 84-0009, 1984.
[5] Saric W., Kozlov V., Levchenko V., Forced and unforced subharmonic resonance in boundary-layer transition, AIAA Paper No. 84-0007, 1984.
[6] Hama F., Some transition patterns in axissymmetric boundary layers, Phys. Fluids 2 (6) (1959) 664–667.
[7] Kovasznay L., Komoda H., Vasudeva B., Detailed flow field in transition, in: Proc. Heat Transfer and Fluid Mech. Inst., Stanford Univ. Press, CA, 1962, pp. 1–26.
[8] Hama F., Nutant J., Detailed flow-field observations in the transition process in a thick boundary layer, in: Proc. Heat Transfer and Fluid Mech. Inst., Stanford Univ. Press, CA, 1963, pp. 77–93.
[9] Knapp C., Roach P., A combined visual and hot-wire anemometer investigation of boundary-layer transition, AIAA J. 6 (1968) 29–36.
[10] Kachanov Y., Kozlov V., Levchenko V., Ramanzanov M., Experimental study of the K-regime breakdown of a laminar boundary layer, Preprint No. 9-84, Inst. Theoret. Appl. Mech., Siberian Div., USSR Acad. Sci., Novosibirsk, 1984 (in Russian).
[11] Saric W., Thomas A., Experiments on the subharmonic route to turbulence in boundary layers, in: Tatsumi T. (Ed.), Turbulence and Chaotic Phenomena in Fluids, North-Holland, Amsterdam, 1984, pp. 117–122.
[12] Kachanov Y., On the resonant nature of the breakdown of a laminar boundary-layer, J. Fluid Mech. 184 (1987) 43–74.
[13] Borodulin V., Kachanov Y., The role of the mechanism of the local secondary instability in K-breakdown of boundary layer, Izv. Sib. Otd. Akad. Nauk SSSR, Ser. Tekh. Nauk. 18 (1988) 65–77 (in Russian). Transl. Sov. J. Appl. Phys. 3 (2) (1989) 70–81.
[14] Borodulin V., Kachanov Y., Experimental study of soliton-like coherent structures in a boundary layer, in: Proc. Scientific and Methodological Seminar on Ship Hydrodynamics, 19th Session, Bulg. Ship Hydrodyn. Cent., Varna, 1990, pp. 99-1–99-10.
[15] Dryganets S., Kachanov Y., Levchenko V., Ramanzanov M., Resonant flow randomization in the K-regime of boundary layer transition, A. Prikl. Mekh. Tekh. Fiz. 2 (1990) 83–94 (in Russian). Transl. J. Appl. Mech. Tech. Phys. 31 (2) (1990) 239–49.
[16] Borodulin V., Kachanov Y., Experimental study of nonlinear stages of boundary-layer breakdown, in: Lin N., Buter T., Reed H. (Eds), Nonlinear Stability of Nonparallel Flows, IUTAM Symp., Potsdam, NY, USA, Springer, 1993.
[17] Borodulin V., Kachanov Y., Formation and development of coherent structures in a transitional boundary layer, J. Appl. Mech. Tech. Phys. 36 (4) (1995) 60–97.
[18] Craik A., Nonlinear resonant instability in boundary layers, J. Fluid Mech. 50 (1971) 393–413.
[19] Craik A., Wave interaction and fluid flows, Cambridge University Press, 1985.
[20] Nayfeh A., Nonlinear stability of boundary layers, AIAA Paper No. 87-0044, 1987.
[21] Herbert T., Secondary instability of boundary layers, Annu. Rev. Fluid Mech. 20 (1988) 487–526.
[22] Rist U., Numerische Untersuchung der räumlichen, dreidimensionalen Störungsentwicklung bei Grenzschichtumschlag, Dissertation, Inst. A Mech. Univ. Stuttgart, 1990.
[23] Kleiser L., Zang T., Numerical simulation of transition and transition in wall-bounded shear flows, Annu. Rev. Fluid Mech. 23 (1991) 493–537.
[24] Kachanov Y., Ryzhov O., Smith F., Formation of solitons in transitional boundary layers: theory and experiments, J. Fluid Mech. 251 (1993) 273–297.
[25] Kachanov Y., Physical mechanisms of laminar boundary-layer transition, Annu. Rev. Fluid Mech. 26 (1994) 411–482.
[26] Rist U., Fasel H., Direct numerical simulation of controlled transition in a flat-plate boundary layer, J. Fluid Mech. 298 (1995) 211–248.
[27] Rist U., Kachanov Y., Numerical and experimental investigation of the K-regime of boundary-layer transition, in: Kobayashi R. (Ed.), Laminar-Turbulent Transition, IUTAM Symp., Sendai, Japan, 1994, Springer, 1995.
[28] Kachanov Y., Levchenko V., The resonant interaction of disturbances at laminar-turbulent transition in a boundary layer, J. Fluid Mech. 138 (1984) 209–247.
[29] Corke T., Mangano R., Resonant growth of three-dimensional modes in transitioning Blasius boundary layers, J. Fluid Mech. 209 (1989) 93–105.
[30] Corke T., Three-dimensional mode growth in boundary layers with tuned and detuned subharmonic resonance, Philos. T. Roy. Soc. A 1700 (1995) 453–471.
[31] Corke T., Gruber S., Resonant growth of three-dimensional modes in Falkner–Skan boundary layers with adverse pressure gradients, J. Fluid Mech. 320 (1996) 211–233.

[32] Bake S., Kachanov Y., Fernholz H., Subharmonic K-regime of boundary-layer breakdown, in: Henkes R., van Ingen J. (Eds), Transitional Boundary Layers in Aeronautics, North-Holland, Amsterdam, 1996, pp. 81–88.
[33] Smith F., Stewart P., The resonant-triad nonlinear interaction in boundary-layer transition, J. Fluid Mech. 179 (1987) 227–252.
[34] Fasel H., Numerical simulation of instability and transition in boundary layer flows, in: Arnal D., Michel R. (Eds), Laminar Turbulent Transition, Springer, Heidelberg, 1990, pp. 587–598.
[35] Goldstein M., Interaction of oblique instability waves with a nonlinear plane wave, J. Fluid Mech. 264 (1994) 343–372.
[36] Volodin A., Zelman M., Three-wave resonant interaction of disturbances in a boundary layer, Izv. Akad. Nauk SSSR, Mekh. Zhidk. Gaza 5 (1978) 78–84 (in Russian).
[37] Zelman M., M., Maslennikova I., On the effects of wave disturbance resonant interaction in a boundary layer, Izv. Akad. Nauk SSSR, Mekh. Zhidk. Gaza 4 (1984) 23 (in Russian).
[38] Herbert T., Subharmonic three-dimensional disturbances in unstable plane shear flow, AIAA Paper No. 83-1759, 1983.
[39] Corke T., Effect of controlled resonant interactions and mode detuning on turbulent transition in boundary layers, in: Arnal D., Michel R. (Eds), Laminar-Turbulent Transition, IUTAM Symp., 1989, Springer, Berlin, 1990, pp. 93–150.
[40] Kloker M., Direkte numerische Simulation des laminar-turbulenten Strömungsumschlages in einer stark verzögerten Grenschicht, Ph.D. thesis, University Stuttgart, Institute of Aero- and Gasdynamics, 1993.
[41] Laurlen E., Kleiser L., Numerical simulation of boundary-layer transition and transition control, J. Fluid Mech. 199 (1989) 403–440.
[42] Gaponenko V., Kachanov Y., New methods of generation of controlled spectrum instability waves in boundary layers, in: Proc. ICMAR, Part 1, Inst. Theor. and Appl. Mech., Novosibirsk, 1994, pp. 125–130.
[43] Barry M., Ross M., The flat plate boundary layer. Part 2. The effect of increasing thickness on stability, J. Fluid Mech. 43 (1970) 813–818.